

Gearbox Vibration Source Separation by Integration of Time Synchronous Averaged Signals

Guicai Zhang and Joshua Isom

United Technologies Research Center, East Hartford, CT 06108, USA

zhangg@utrc.utc.com

isomjd@utrc.utc.com

ABSTRACT

This paper describes a simple approach for integrating all the time synchronous average (TSA) signals from multiple shafts of a gearbox to generate a composite time synchronous average which can be subtracted from the original signal to generate a second-order cyclostationary residual. This approach is compared with other techniques including an all-shaft TSA over the least common multiple of shaft rotation periods, high-pass filtering, and self-adaptive noise cancellation (SANC). The results demonstrate that the proposed approach produces an integrated TSA signal that includes only the shaft components, gear mesh components and the sidebands associated with all the shafts, while the residual contains the random vibration components and noise. The results produced by three alternative techniques do not separate the components as well or have a lower signal-to-noise ratio.*

1. INTRODUCTION

Gearboxes are an important component in a wide variety of machinery including helicopters, wind turbines, aero-engines, and automobiles. Gearboxes tend to be complex with ever increasing needs of power transmission, speed change and compact size of modern equipments. A complex gearbox (e.g., the planetary gearboxes used in wind turbines and helicopters) may have several dozen gears, as many bearings, and five or more shafts rotating at different speeds. Failures in any of the components may cause the malfunction of the entire gearbox and the maintenance or replacement of the gearbox is of very high cost.

Fault diagnostics, prognostics and health management (PHM) for gearboxes is a great challenge and has attracted a lot of attention for the past over

thirty years (Welbourn, 1977; Randall, 1982; McFadden, 1986). The separation of vibration sources in a complex gearbox is critical for effectively and accurately diagnosing gearbox failures. Due to the complexity of the gearbox, there are typically more vibration sources than sensors; thus the use of fully determined source-separation techniques like independent component analysis (ICA) is limited.

In this work, we propose a source separation method based on the single shaft TSA. Specifically, it integrates the TSA components from each shaft and produces a composite signal including vibration sources from all the shafts and gears. When the resulting composite signal is subtracted from the original signal, one obtains a residual signal that contains the vibration components from bearings and random noise. The paper is organized as follows. Section 2 is a brief review of existing work on gearbox vibration source separation. Section 3 describes the algorithm for the proposed method and a demonstration using gearbox vibration data. Section 4 provides a justification for the proposed algorithm. Section 5 compares the source separation results obtained by the proposed method with those produced by other existing techniques. Section 6 and Section 7 contain a discussion and conclusion.

2. BRIEF REVIEW OF GEARBOX VIBRATION SOURCE SEPARATION TECHNIQUES

Vibration monitoring is the most widely used health-monitoring method for gearbox and other rotating machinery. A basic source separation technique long employed for gearbox health monitoring is the time synchronous average. The time synchronous average extracts periodic waveforms from a vibration mixture by averaging the vibration signal over several revolutions of the shaft of interest. This can be done in either the time or frequency domain. The time synchronous average technique enhances vibration features that are synchronous with a particular shaft, and attenuates features that are not synchronous with that shaft. The technique has proved to be useful for monitoring of gear and shaft health.

* This is an open-access article distributed under the terms of the Creative Commons Attribution 3.0 United States License, which permits unrestricted use, distribution, and reproduction in any medium, provided the original author and source are credited.

Techniques for the separation of bearing vibration from other gearbox vibration sources are also available. The high-frequency resonance technique is one specifically designed for extracting features of local defects in bearings.

Adaptive noise cancellation (ANC) can be used to extract a faulty bearing signal in cases where the primary signal can be measured near the faulty bearing of a gearbox, and a secondary reference signal measured near another remote healthy bearing is also available. When one of the two components to be separated is deterministic (gear and shaft signals) and the other random (bearing signal), the reference signal can be made a delayed version of the primary signal. This is based on the fact that the random signal has a short correlation length while deterministic signal has long correlation length. Thus the adaptive filter will find the transfer function between the deterministic part of the signal and the delayed version of itself. The separation of the deterministic and random parts can also be achieved using one signal only, and this technique is called self-adaptive noise cancellation (SANC). The performance of the SANC algorithm depends on the choice of three parameters: the time delay, the filter length and the forgetting factor (Antoni and Randall, 2004, Zeidler, 1990). In practice, there are trade-offs between the parameter settings and signal properties such as the length of the measured signal.

Independent component analysis (ICA) is a standard technique for blind source separation. It has been applied to separate signals from two independent vibration sources recorded at two separate locations on a gearbox (Zhong-sheng, et al., 2004). The utility of this technique is limited to cases where the number of sensors is equal to or greater than the number of vibration sources, a condition that does not generally hold for gearbox vibration monitoring.

Principal component analysis (PCA) has also been used to identify the number of gearbox vibration sources (Gelle et al., 2003, Serviere et al., 2004). The utility of this dimensionality-reduction technique is limited by the fact that the reduced-dimension vibration features may not have physical significance and thus it is difficult to create a mapping between features and physical vibration sources.

3. THE INTEGRATED TIME SYNCHRONOUS AVERAGE

Although the TSA is a powerful tool for isolating gear and shaft components synchronous with a particular shaft, it fails to isolate random vibration components because the subtraction of a single TSA from the original signal results in a combination of random signals and other shaft-synchronous components.

A natural way to deal with the issue of separating shaft/gear components from random signals is to extend the standard single-shaft TSA to multiple shafts by conducting an average over the least common multiple of shaft rotation periods to include the components associated with all the shafts. Thus the residual only contains random components with the exclusion of the deterministic parts. However, this technique is impractical because the time period corresponding to the least common multiple of the shaft revolutions for an actual gearbox is usually several hours.

Recently, two methods have been described for subtracting a composite TSA from a vibration signal to produce a residual signal (Randall and Antoni, 2011). A frequency domain method consists of computing the FFT of the entirety of a signal, and simply removing spectral peaks at the discrete harmonics of the known periodic signals.

A second method, a time domain method, consists of multiple resampling and subtraction of time synchronous averages from a signal (Randall and Antoni, 2011).

Both of these issues have shortcomings. The frequency-domain approach must deal with the fact that the frequency of the harmonics leaks into adjacent bins, except for the very special case in which the numbers of sample per period and the number of periods are powers of two. In the case where there is leakage, removal of discrete peaks at shaft harmonics will not completely remove the periodic signal.

The time-domain approach described in (Randall and Antoni, 2011) has the issue that there are certain time-domain features that are common to the time synchronous average of two or more shafts – the signal corresponding to the gear mesh frequency being a universal example. Thus, repeated subtraction of individual TSAs will “over-subtract” certain features of the periodic signals.

In this work, an alternative method is proposed to integrate all the single shaft TSA signals to obtain a combination of the components synchronous with each shaft in a gearbox. The proposed method overcomes the limitations of the existing methods based on a time synchronous average, is simple, and performs better than other techniques not based on the time synchronous average.

The new algorithm is presented in Table 1 and justified in Section 4. To obtain the integration of the TSAs, all the single shaft TSA signals should have the same number of data points (this is actually the same spatial angle of one chosen reference shaft after angular resampling), and this can be achieved by interpolating and/or repeating the TSA time series. An FFT is then applied to each of the TSAs to get a complex series in the Fourier domain. Next, the magnitudes of each complex series are computed and a new series with the

same length is formed by taking the complex value which has the maximum magnitudes of all the single shaft TSA signals. The maximum magnitude series is used to create a time series using an inverse FFT operation. The new time series contains all the shaft components, mesh frequencies and their sidebands, and we call it the *integrated TSA*. A residual signal can be obtained by subtracting the integrated TSA from the original signal.

-
1. Read the original vibration data and tachometer data.
 2. Conduct TSA for each shaft: $Tsa1, Tsa2, Tsa3, \dots$
 3. Interpolate and repeat data to obtain $TSA1, TSA2, TSA3, \dots$, of the same length N .
 4. FFT to get complex series: $C_{TSA1} = \text{fft}(TSA1), C_{TSA2} = \text{fft}(TSA2), C_{TSA3} = \text{fft}(TSA3), \dots$
 5. Compute magnitude series: $A_{TSA1} = \text{abs}(C_{TSA1}), A_{TSA2} = \text{abs}(C_{TSA2}), A_{TSA3} = \text{abs}(C_{TSA3}), \dots$
 6. Obtain maximum magnitude series: $MaxA_{TSA} = \max(A_{TSA1}, A_{TSA2}, A_{TSA3}, \dots)$
 7. For $i = 1:N$
 - if $A_{TSA1}(i) == MaxA_{TSA}(i)$
 - $C_{Total}(i) = C_{TSA1}(i)$
 - elseif $A_{TSA2}(i) == MaxA_{TSA}(i)$
 - $C_{Total}(i) = C_{TSA2}(i)$
 - elseif $A_{TSA3}(i) == MaxA_{TSA}(i)$
 - $C_{Total}(i) = C_{TSA3}(i)$
 -
 - end
 - End
 8. Inverse FFT: $TC_{Total} = \text{iFFT}(C_{Total})$
 9. Integrated TSA time waveform = $\text{real}(TC_{Total})$
-

Table 1. Integrated TSA algorithm

4. ALGORITHM JUSTIFICATION

The objective of the time synchronous average is to extract a periodic signal synchronous with a particular shaft from a mixture of signals. If $y(t)$ is a signal that is periodic with period T , then it can be represented with the Fourier series expansion

$$y(t) = a_0 + \sum_{n=1}^{\infty} \left(a_n \cos \frac{n\pi t}{T} + b_n \sin \frac{n\pi t}{T} \right) \quad (1)$$

Conceptually, the objective of the time synchronous average is to extract only those portions of the signal that have frequency $\frac{n\pi}{T}$, $n = 1, \dots, \infty$.

In actuality, the time synchronous average consisting of the average of N periods for a signal with period T is equivalent to a comb filter with a frequency response given by $|H(f)| = \frac{1}{N} \frac{\sin(\pi N f T)}{\sin(\pi f T)}$ (Braun, 2011), which is plotted in Figure 1 as a function of f/T . The lobes of the comb filter naturally address the leakage issue. As N becomes large, the lobes of the filter become more tightly centered on the frequencies

$$f = \frac{n\pi}{T}, n = 1, \dots, \infty. \quad (2)$$

A filter selective for K periodic components corresponding to different shafts, each with period T_i , should be selective for the frequencies

$$f = \frac{n\pi}{T_i}, n = 1, \dots, \infty; i = 1, \dots, K. \quad (3)$$

This filter should be windowed to address leakage. Such a filter can be formed by merging multiple comb filters with a maximum-select rule,

$$|H(f)| = \max_i \left\{ \frac{1}{N_i} \frac{\sin(\pi N_i f T_i)}{\sin(\pi f T)} \right\}. \quad (4)$$

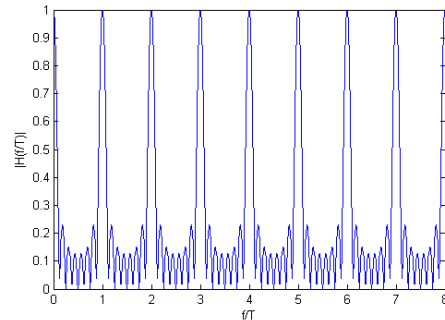


Figure 1. Frequency response of a comb filter equivalent to the time-synchronous average, as a function of f/T

The spectrum of this maximum-select comb filter is equivalent to the spectrum produced by Step 7 of the algorithm presented in Table 1. The maximum-select algorithm is actually equivalent to that selection of one of the non-zero complex values from the FFT series of the single-shaft TSAs along the frequency axis. This operation avoids producing redundant components in the integrated TSA.

5. EXPERIMENT

5.1 Application to Gearbox Vibration Data

In this section, the integrated TSA method described above is applied to vibration signals collected from a two-stage gearbox. This method is also compared with other source separation techniques, namely, the all-shaft TSA in which an average is conducted over the least common multiple of shaft revolutions; high/low-pass filtering; and self-adaptive noise cancellation (SANC).

5.2 Data

The data used for the demonstration of the proposed method is from the 2009 PHM Challenge.

The gearbox has three shafts (an input shaft, an idler shaft, and an output shaft), each with input side and output side bearings, and a total of four gears, one on the input shaft, two on the idler shaft, and one on the output shaft. During the experiments, a tachometer signal was collected from the input shaft with 10 pulses per revolution and two accelerometers were mounted on the input side and output side to collect vibration acceleration signals. The gear mesh configuration and sensor locations are illustrated in Figure 2.

For the method demonstration, selected data sets from the 2009 PHM Challenge were used. The data sets collected from the gearbox include both spur gear pair and helical gear pair configuration. The operating condition for the data sets used in this paper was the spur gear configuration, operating at high torque, with an input shaft speed is 3000 rpm (50Hz). The number of teeth for the two spur gear pairs are 32/96 and 48/80, respectively. The sampling frequency is 66.667 kHz and the sampling period is about 4 seconds for each data set.

The feature frequencies of the shafts and gears are listed as follows: the 1st and the 2nd mesh frequency are 1598 Hz and 799 Hz respectively, and the three shaft frequencies are 50 Hz, 16.7 Hz, and 10 Hz for the input, idler, and output shafts, respectively.

5.3 Demonstration of the integrated TSA method

In the following the results were generated from data set Spur 3 in which the gear of 48 teeth on the idler shaft is eccentric.

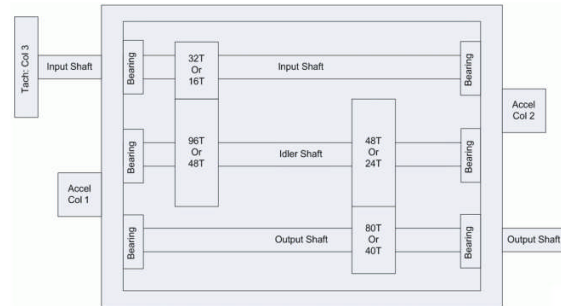


Figure 2. Configuration of the testing gearbox

Figure 3 shows the single shaft TSA waveforms for the input shaft, idler shaft and the output shaft (one revolution for each shaft), respectively. The corresponding time periods for the three shafts are different due to the different rotation speeds of the shafts. The eccentric feature is clearly evident in the TSA waveform of the idler shaft.

Figure 4 shows the original time waveform of the same acceleration signal (Spur 3), the integrated TSA waveform and the residual waveform.

Figure 5 shows magnitude spectra corresponding to the time waveforms shown in Figure 4. Only the frequency range below 2000 Hz is shown which covers the lower orders of the shaft harmonics, the two mesh frequencies (1598 Hz and 799 Hz) and their sidebands in Figure 5. From Figure 5 it can be seen that in the residual signal the shaft components and the gear mesh components are removed or attenuated significantly. It can also be seen from the magnitude spectrum of the original signal that the peak at the second mesh frequency (799 Hz) is significantly larger than that of the first mesh frequency (1598 Hz), and the peak at the input shaft frequency (49.9 Hz) is also one of the dominant components. The spectrum of the integrated TSA basically contains the shaft frequencies and their harmonics, as well as the mesh frequencies with the sidebands from the three shafts, and this can be seen most clearly in the following zoomed-in plots.

Figure 6 provides a comparison of the spectra of the original signal, the integrated TSA, and the residual signal at lower frequency band. From Figure 6 it can be seen that the integrated TSA basically contains the harmonics of the three shafts and in the residual signal the major periodic components (mainly the three shaft frequencies and their harmonics) are removed.

Figure 7 show the spectral comparison between the original signal and the integrated TSA zoomed-in around the two mesh frequencies. From Figure 7 it can be seen that the integrated TSA mainly contains the mesh frequencies and the sidebands associated with all the three shafts. And the dominant sidebands are caused by the idler shaft on which there is an eccentric gear.

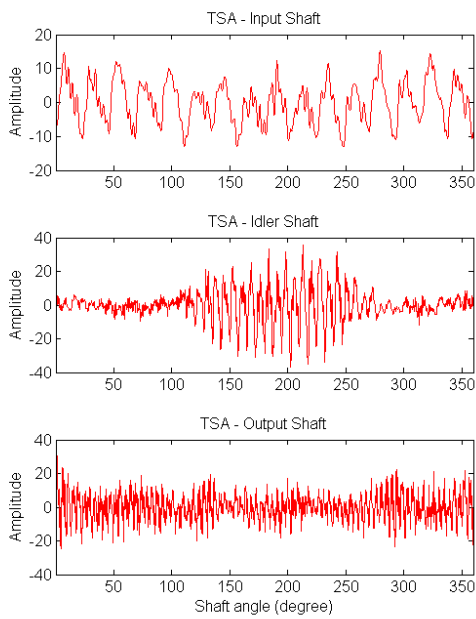


Figure 3. Single-shaft TSA waveforms

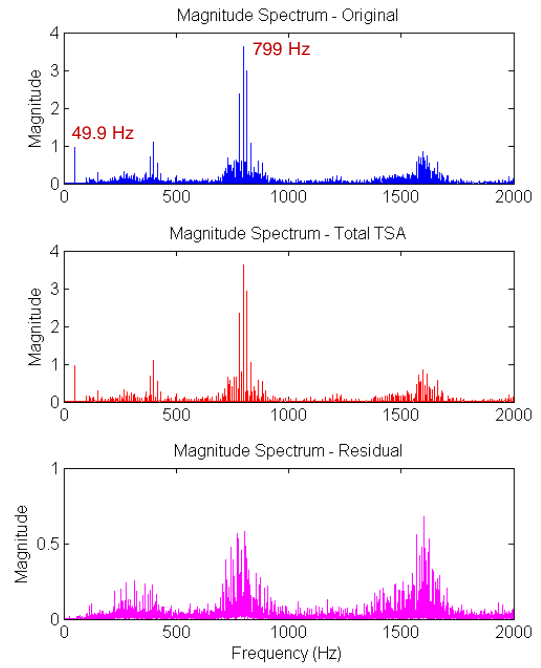


Figure 5. Magnitude spectra of the signals shown in Figure 4

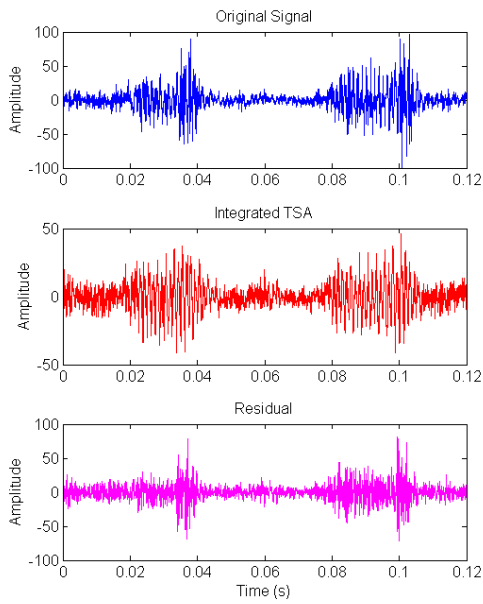


Figure 4. Waveforms for the original signal, the integrated TSA, and the residual

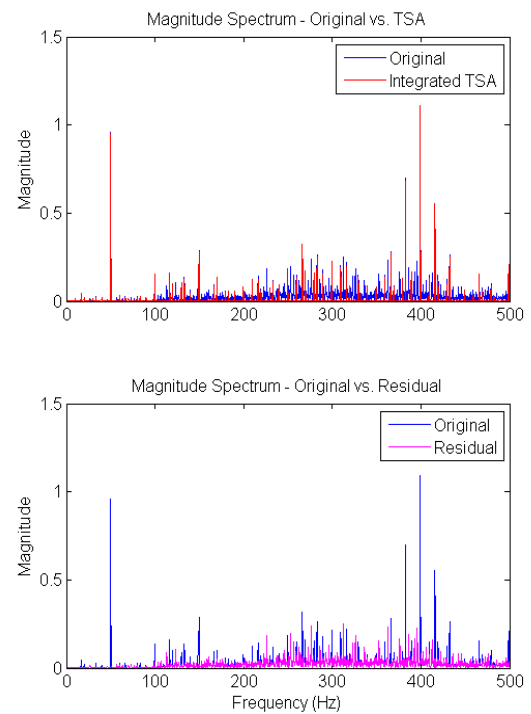


Figure 6. Spectrum comparison at lower frequency band

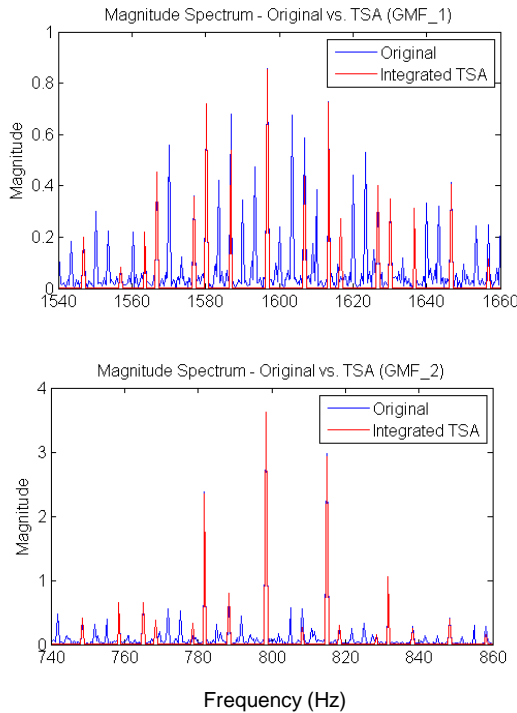


Figure 7. Spectrum comparison around the two gear mesh frequencies

5.4 Comparison with other techniques

In this section, the integrated TSA is compared with other techniques, namely, all-shaft TSA, high/low-pass filtering and SANC, using data from the PHM 2009 Challenge.

In these comparisons, data set Spur 6 with a rotation speed of 3000 rpm for the input shaft and a high load condition is used. There are some compound faults seeded in this data set, specifically, a broken tooth on the gear (80 teeth) installed on the output shaft, a defect on the bearing inner race, a ball defect, and an outer race defect in the bearings supporting the input side of the input shaft, idler shaft and the output shaft respectively. The input shaft is also imbalanced.

The cut-off frequency used in the high/low-pass filtering method is set to 5000 Hz which is roughly equal to three times the gear mesh frequency of 1598 Hz plus the fourth order sideband of the input shaft frequency 50 Hz (the highest shaft frequency among the three shafts).

Figure 8 shows the time-domain waveform of the data set, which evidences strong impulses caused by the broken tooth.

Figure 9 shows the magnitude spectrum of the original signal. From Figure 9 it is seen that the rotation frequency of the input shaft is the dominant component for this data set and has a much higher magnitude than the gear mesh vibration components.

Figure 10 (a), (b), (c) and (d) show the separated periodic components and the random transient components produced by the integrated TSA, all-shaft TSA, high/low-pass filtering and SANC, respectively. From Figure 10 it can be seen that the results from the separated results by using integrated TSA and all-shaft TSA look very close to each other. The other two methods -- high/low-pass filtering and SANC -- cannot filter out the broadband impulses from the periodic portion of the signal. One also notes some over-attenuation at the start of the filtered signal in the results of the SANC.

Figure 11 (a), (b), (c) and (d) provides a comparison of the magnitude spectra of the separated components in the lower frequency bands (<500Hz). It can be seen that the all-shaft TSA includes a more components than that of the integrated TSA in the low frequency band, while in the filtered parts of the other two filtering approaches almost all the components in low frequency bands are kept. The magnitudes of the residual spectra for high/low-pass filtering and SANC are close to zero, while some larger peaks (random components) could be found in the residual spectra of the integrated TSA and all-shaft TSA.

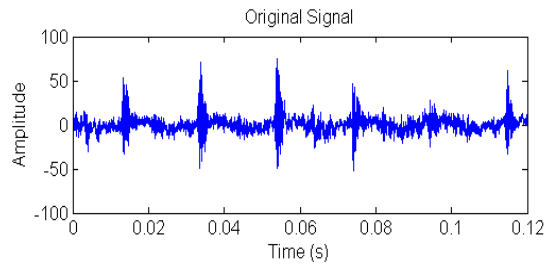


Figure 8. Original time waveform (Spur 6)

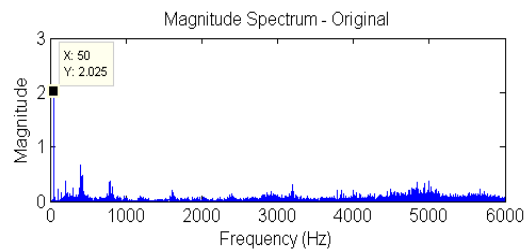
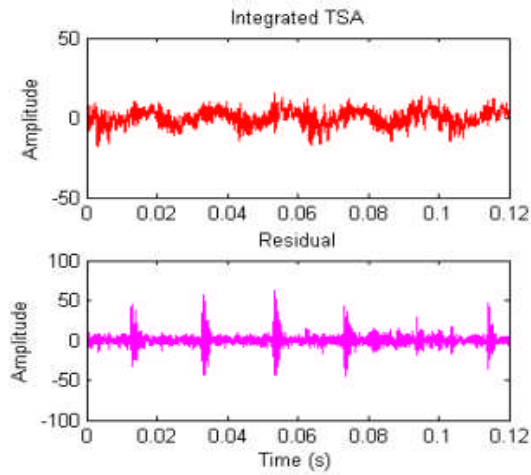
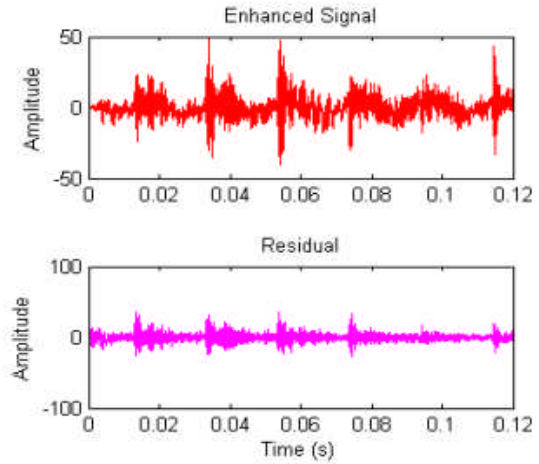


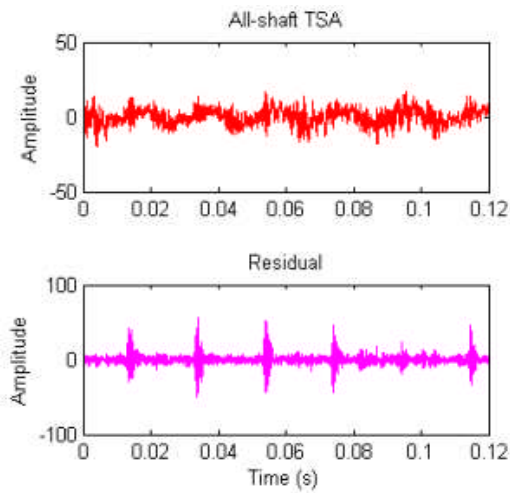
Figure 9. Magnitude spectrum of the original signal (Spur 6)



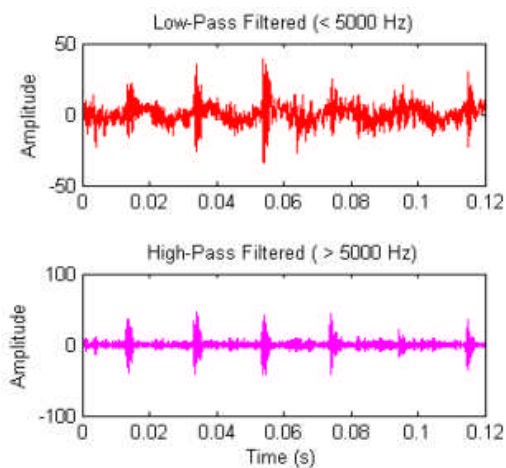
(a) Integrated TSA



(d) SANC



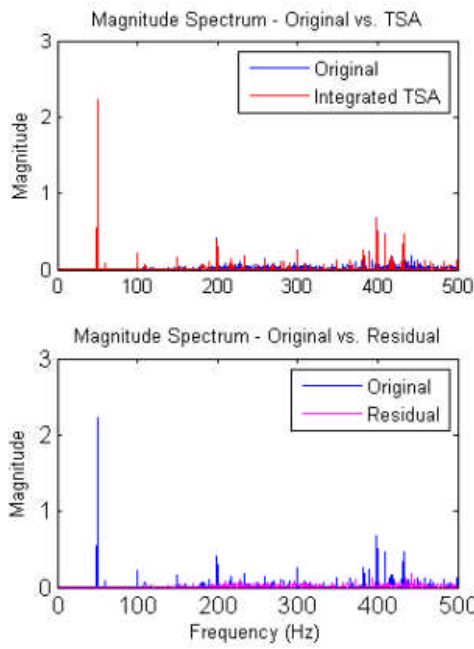
(b) All-shaft TSA



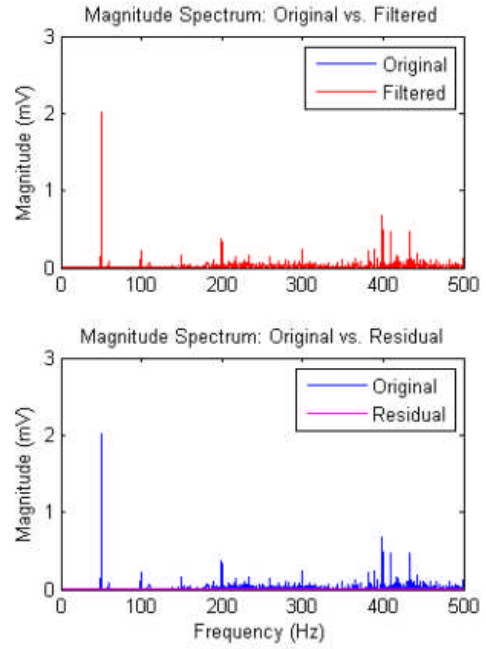
(c) High-Pass filtering

Figure 10. Comparison of the separated signals

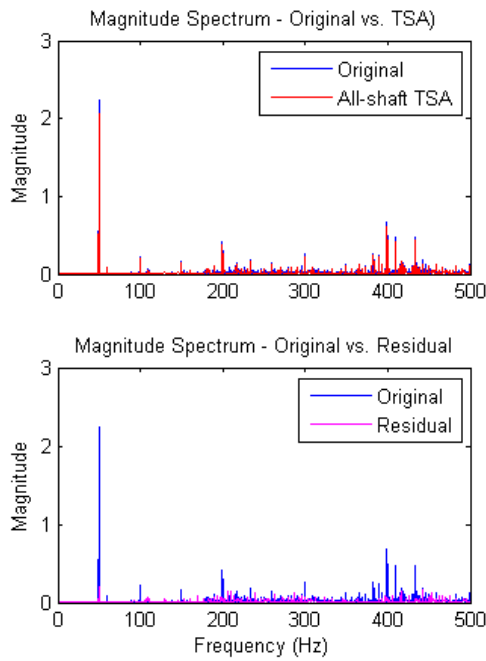
Figure 12 provides a comparison of the magnitude spectra of the separated components for the integrated TSA, all-shaft TSA and SANC methods around the second gear-pair mesh frequency ($GMF2 = 799$ Hz). And Figure 13 provides a comparison of the magnitude spectra of the separated components for the integrated TSA, all-shaft TSA and SANC methods around the first gear-pair mesh frequency ($GMF1 = 1598$ Hz). The result of high-pass filtering are not shown here as the cut-off frequency of 5000 Hz is much higher than these frequency bands and thus all the original components are kept in the filtered signals and the magnitudes of the residual signals are basically zero in the frequency bands compared here. It can be seen from Figure 12 and Figure 13 that the integrated TSA contains the mesh frequencies and their sidebands from all three shafts. The all-shaft TSA includes more periodic components than that of the integrated TSA and it is seen that there are some peaks between the mesh frequencies and the sidebands in the all-shaft TSA spectrum. From the spectrum of the filtered signal by SANC, it is seen that it covers all the major peaks and its residual signal is of very small magnitudes. It can also be seen from these spectra that the residual is complementary with the TSA or filtered signal to form the original signal, as expected.



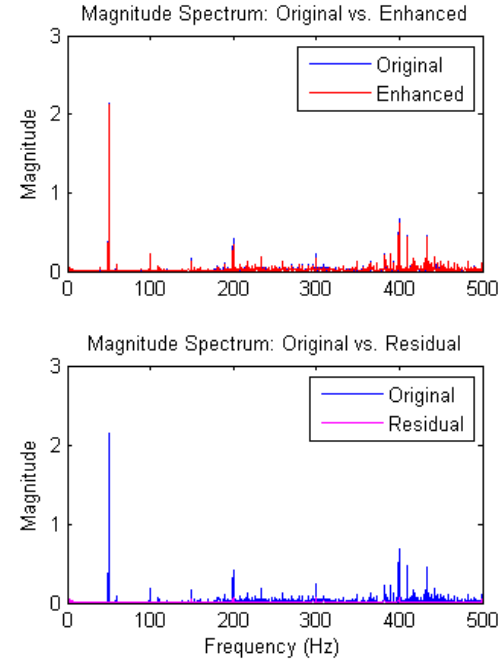
(a) Integrated TSA



(c) High-Pass filtering

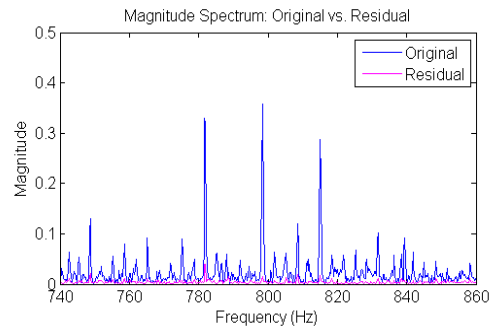
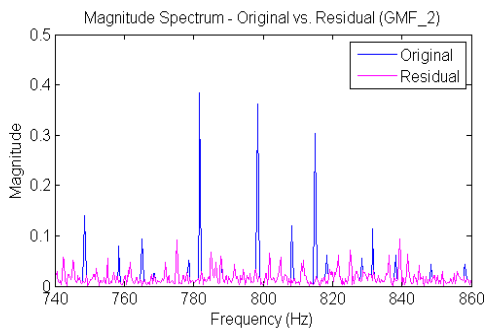
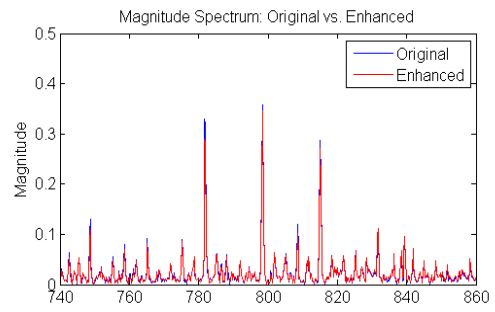
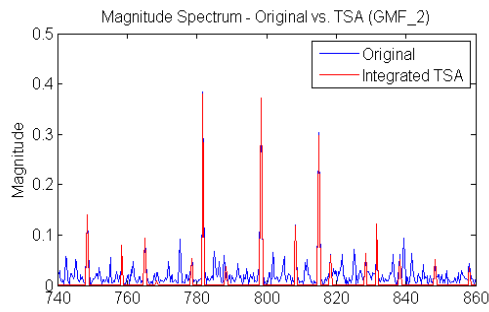


(b) All-shaft TSA



(d) SANC

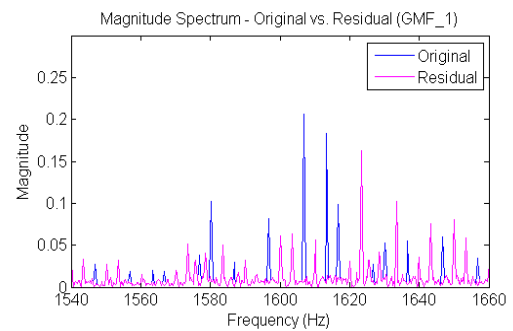
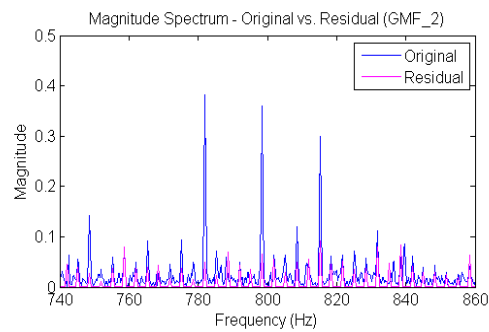
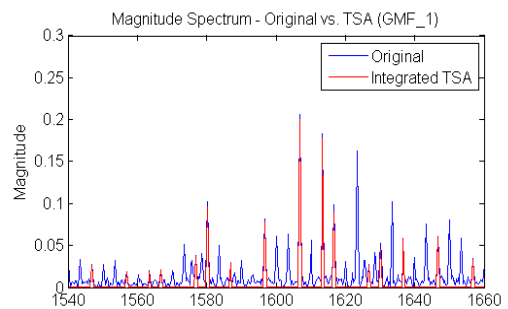
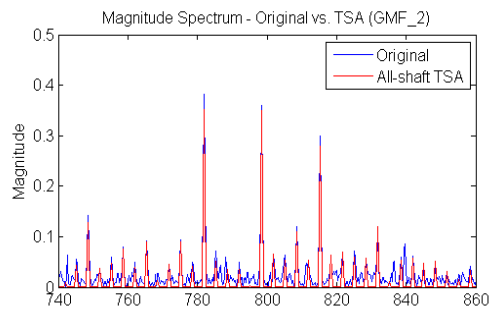
Figure 11. Spectrum comparison of the separated signals (in low frequency bands)



(a) Integrated TSA

(c) SANC

Figure 12. Spectrum comparison of the separated signals (zoomed in around GMF2)



(b) All-shaft TSA

(a) Integrated TSA

Figure 13. Spectrum comparison of the separated signals (zoomed in around GMF1)

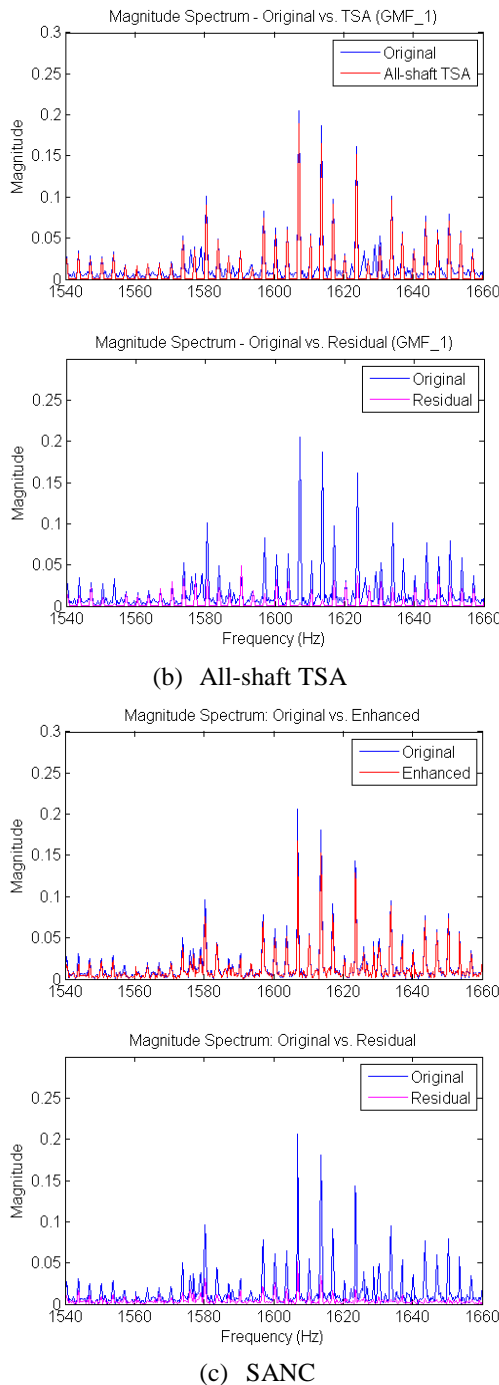


Figure 13 (continued). Spectrum comparison of the separated signals (zoomed in around GMF1)

6. DISCUSSION

Based on the analysis results in the above section, the following observations can be made:

1. The integrated TSA keeps all the shaft synchronous components including the shaft rotation frequencies and their harmonics, gear mesh frequencies and their harmonics with the sidebands from all the shafts. Vibration components other than these are significantly attenuated or eliminated.

2. The all-shaft TSA includes more vibration components than the integrated TSA. There are basically two reasons for this: (a) averaging over the least common multiple of the shaft revolutions includes the components with period of the least common multiple of the periods of the shafts (the peaks between the mesh frequencies and the shaft sidebands); (b) averaging over longer period also makes the number of averages smaller and this makes the signal-to-noise ratio lower (equivalent to higher side lobes of the comb filter). The data used in this paper is a special case in which all-shaft TSA can be applied. However, as mentioned in Section 3, for industrial gearboxes the least common multiple of the shaft revolution periods is usually several hours, making the technique impractical.

3. The high/low-pass filtering method separates the data according to the frequency range. Ideally the low frequency part should include the vibration components of the shafts and the gear mesh. However, the low frequency part surely includes all the periodic components not associated with the shafts and gears and noise components in the frequency bands lower than the cut-off frequency.

4. The filtered part of SANC is determined by the time delay factor, forgetting factor, and filter length. These should be optimized with the specific data type and data length to reach some trade-offs and in practice this is somewhat arbitrary and difficult to obtain satisfactory results.

5. Both high/low pass filtering and SANC fail to filter out broadband impulses. The transient feature is clearly seen in the deterministic part.

7. CONCLUSIONS

This paper describes a simple approach for integrating the TSA of individual shafts to generate a composite time synchronous average which can be subtracted from the original signal to generate a second-order cyclostationary residual. This approach is applied to vibration signals collected from a two-stage gearbox and compared with other techniques including an all-shaft TSA in which angular re-sampling over the least common multiple of shaft revolutions is conducted, high/low pass filtering and self-adaptive noise cancellation.

The results demonstrate that by using the proposed approach, the integrated parts contain only the components synchronous with each of the shafts

including the shaft frequencies and their harmonics, mesh frequencies and their harmonics, and the sidebands caused by all the shafts around the harmonics of the mesh frequencies. The all-shaft TSA signal contains more components than that of synchronous with each shaft and has a lower signal-to-noise ratio than the integrated TSA. High/low pass filtering and SANC induce more noise in the filtered part and the results are less satisfactory.

The integrated TSA is a simple but powerful approach for the separation of a gearbox vibration signal into first-order and second-order cyclostationary components. The new technique will facilitate the diagnosis of faults in complex gearbox systems.

REFERENCES

- Antoni, J., Randall, R.B. (2004). Unsupervised noise cancellation for vibration signals: part I - evaluation of adaptive algorithms, *Mechanical Systems and Signal Processing* 18 (2004) 89–101
- Braun, S. (2011). The synchronous (time domain) average revisited, *Mechanical Systems and Signal Processing*, 25 (2011) 1087-1102
- Gelle, G., Colas, M., Serviere, C. (2003). Blind source separation: a new pre-processing tool for rotating machines monitoring, *IEEE Transactions on Instrumentation and Measurement*, vol. 52, pp. 790-795.
- McFadden, P.D. (1986). Detecting fatigue cracks in gears by amplitude and phase demodulation of the meshing vibration. *ASME Transactions Journal of Vibration, Acoustics, Stress and Reliability in Design* 108, 165–170.
- PHM Challenge 2009 Data Sets:
<http://www.phmsociety.org/references/datasets>
- Randall, R.B. (1982). A new method of modeling gear faults. *ASME Journal of Mechanical Design*, 104, 259–267.
- Randall, R.B., Antoni, J. (2011). Rolling Element Bearing Diagnostics — A Tutorial, *Mechanical Systems and Signal Processing*, 25(2011), 485–520.
- Serviere, C., Fabry, P. (2004). Blind source separation of noisy harmonic signals for rotating machine diagnosis, *Journal of Sound and Vibration*, vol. 272, pp. 317-339.
- Tan, C.C., Dawson, B. (1987). An adaptive noise cancellation approach for condition monitoring of gearbox bearings, *Proceedings of the International Tribology Conference*, Melbourne, 1987.
- Welbourn, D.B. (1977). Gear Noise Spectra - a Rational Explanation, *ASME 1977 International Power Transmission and Gearing Conference*, Chicago, 28-30 Sept 1977
- Zeidler, J.R. (1990). Performance analysis of LMS adaptive prediction filters, *Proceedings of the IEEE*, 1990, 78 (12), 1781–1806.
- Zhong-sheng, C., Yong-min, Y., Guo-ji, S. (2004). Application of independent component analysis to early diagnosis of helicopter gearboxes. *Mechanical Science and Technology*, 2004, 23(4), 481-484.

Guicai Zhang received the M.S. from Xi'an JiaoTong University, Xi'an, China in 1993, the Ph.D. from Huazhong University of Science and Technology, Wuhan, China in 2000, both in Mechanical Engineering. He is a Staff Research Engineer in the area of prognostics and health management at United Technologies Research Center (China). Before joining United Technologies Research Center in 2005, he was an Associate Professor at Shanghai JiaoTong University from 2003 to 2005 and a Research Associate at the Chinese University of Hong Kong from 2000 to 2003.

Joshua D. Isom received the B.S. from Yale University in 2000, the M.S. from Rensselaer at Hartford in 2002 and the Ph.D. from the University of Illinois at Urbana-Champaign in 2009. He is a Principal Engineer in the area of prognostics and health management at United Technologies Research Center. Before joining United Technologies Research Center in 2010, he was the technical lead for prognostics and health management at Sikorsky Aircraft Corporation from 2007 to 2010. He was a lead systems engineer at UTC Power in South Windsor, CT from 2000 through 2007.